

DEVELOPMENT OF SEISMIC DEMAND AND CAPACITY ASSESSMENT METHODOLOGY FOR RECTANGULAR CONCRETE-FILLED STEEL TUBE (RCFT) MEMBERS AND FRAMES

C. Tort¹ and J. F. Hajjar²

ABSTRACT

Accurate assessment of demand and capacity of structures is critical in developing performance-based design methodologies. In this research, new methods are presented towards quantifying demand and capacity of RCFT frames and members. An experimental database was compiled documenting local damage levels of RCFT members. The quantified information collected from the experiments was utilized in calculating the available capacity of RCFT members at multiple performance levels. To assess seismic demand, a 3D corotational mixed fiber-based finite element formulation was derived allowing both geometrically and materially nonlinear analysis of frames made up of RCFT columns and steel girders. This finite element formulation has several unique features designed to capture the main characteristics of RCFT members observed in experimental tests, including slip between the steel tube and concrete core, local buckling of steel tube, and confinement of the concrete. It was implemented in a general purpose finite element program and verified by comparing to the cyclic and monotonic beam-column tests.

Introduction

Rectangular concrete-filled steel tube (RCFT) frames are known for their excellent seismic performance with high ductility and large energy absorption capacity (Hajjar 2002). This is often attributed to the interaction of the steel tube and concrete core. Confinement of concrete provided by the steel tube alleviates the abrupt failure of concrete and also local buckling of the steel tube is delayed due to the restraining action of the concrete media. Therefore, it is important to account for the interaction between steel and concrete in modeling RCFT members. In addition, RCFT members exhibit distinct local damage levels of concrete cracking, concrete crushing, steel tube yielding etc. as reported in (Tort and Hajjar 2004). Prediction of these local damage levels is only possible with accurate modeling of composite nature of RCFT members.

In this research, an experimental database was constructed consolidating worldwide literature on RCFT members and frames. The experimental results documented in the database were later used in quantifying the available local capacity of RCFT members. To conduct studies for the assessment of seismic demand, a new 3D corotational mixed finite element formulation was derived following the past work by (Hajjar et al. 1998) and (White and Nukala

¹ Graduate Research Assistant, Department of Civil Engineering, University of Minnesota, Minneapolis, MN 55455

² Professor, Department of Civil and Environmental Engineering, University of Illinois, Urbana, IL 61801

2003). This finite element formulation has the capability to simulate slip between the steel tube and concrete core. Uniaxial cyclic constitutive models of the steel tube and concrete core were derived to simulate the materially nonlinear response of RCFTs. The finite element formulation was implemented in (OpenSEES 1999) and verified with respect to monotonic and cyclic experimental tests from the literature. Developing a comprehensive computational formulation to analyze RCFT frames both allows researchers to develop, test, and verify new analysis and design methods (e.g., intensity measures, demand measures) for performance-based design and also it helps practitioners use advanced analysis methods (e.g., nonlinear push-over, nonlinear time history) in design to evaluate a wide range of performance objectives with reduced uncertainty.

Development of Experimental Database

Worldwide experimental literature on RCFT members was examined and the specimens of well reported tests were included in the database. The specimens were classified as columns, beam-columns, pinned-connections, panel zones, and frames depending on the test setup and loading conditions. The database contained information about the geometric dimensions and material properties of the specimens. In addition, experimental results of the specimens were reported covering information about load and deformation capacities, failure modes, and occurrence of local damage levels in terms of their load and deformation values. Using experimental results in the database, damage function equations were derived to estimate the available capacity of the specimens at multiple performance levels (Tort and Hajjar 2004).

Finite Element Formulation

In performance-based design, capacity and demand of frame structures are often quantified through conducting a series of nonlinear time history analyses. However, the prerequisite of this stage is to develop a finite element model that is capable of representing the key features of RCFT members under static loading applied either monotonically or cyclically.

An 18 DOF beam-column finite element was formulated to model RCFT members based on the past work by (Hajjar et al. 1998). In this model, the translational degree of freedoms of steel tube and concrete core are defined separately creating 3 additional degrees of freedom at each joint. This approach allows differential movement of steel tube and concrete core. Since concrete core is placed inside steel tube, shear deformation compatibility is ensured through utilizing penalty functions between shear translational DOFs of steel tube and concrete core. This results in differential movement between steel tube and concrete core only in the axial direction. The DOFs of the RCFT beam-column finite element are numbered in a manner that allowed automated assembly of 12 DOF steel beam elements into 18 DOF RCFT beam-column elements in a composite frame. When a steel girder frames into an RCFT column, the DOFs of the steel girder are assembled into the first 6 DOFs of the RCFT joint, which corresponds to the steel tube DOFs. The last 3 DOFs of the RCFT joints are defined for concrete translations, and the nodal forces from steel girder are transferred to the concrete core through the slip interface between the steel tube and concrete core. The slip response of RCFT beam-column elements was calibrated with respect to push-out tests and connections tests available in the literature by (Hajjar et al. 1998). A bond strength of 0.087 ksi was assumed and a bilinear slip vs. bond strength response was adopted with an initial stiffness (k_{sc}) of 1450 ksi defined around the

perimeter of the steel tube.

In this research, the RCFT beam-column finite element by (Hajjar et al. 1998) was augmented by implementing a new mixed finite element-based state determination scheme following the work by (Nukala and White 2003). The mixed finite element formulations are known to have better accuracy with a coarse mesh as compared to equivalent displacement-based formulations due to the fact that in mixed formulations curvature distribution along the element length can be estimated more accurately (Nukala and White 2003). In addition, in mixed formulation, equilibrium along the element length is strictly enforced while it is satisfied only in the variational sense in displacement-based formulations. Equilibrium of element forces alleviates numerical difficulties arising from concrete cracking (Hajjar et al. 1998).

The proposed state determination methodology follows the Hellinger-Reissner two-field variational principle, where displacement fields and forces fields are interpolated independently. The element internal forces (Q) are calculated by satisfying the element equilibrium, displacement compatibility, and cross-section equilibrium given in Eqs. 1, 2 and 3, respectively (symbols not defined in the text are defined in the Appendix; the left superscript in the symbols below identifies the configuration in which a quantity is measured while left subscript identifies the reference state; “1” denotes the last converged configuration (C1) and “2” denotes the current configuration (C2); L is the element length; “ δ ” identifies the variation):

$$\int_0^L \delta_1^2 \hat{d}_{.1}^2 D . dx + \int_0^L \delta_1^2 \hat{d}_{sc .1}^2 D_{sc} . dx - \delta_1^2 q^T .^2 Q_{ext} \quad (1)$$

$$\int_0^L \delta_1^2 D^T . (^2 d - ^2 \hat{d}) . dx = 0 \quad (2)$$

$$^2 D - ^2 D_{\Sigma} = 0 \quad (3)$$

The second term in Eq. 1 accounts for the energy due to slip taking place between steel tube and concrete core. The state determination algorithm adopted in this research involves solution of compatibility and cross-section equilibrium equations linearly. The unbalance of compatibility and cross-section equilibrium are converted into unbalanced nodal forces and they are eliminated in global Newton-Raphson iterations.

The state determination process starts by solving for the nodal displacements (q) corresponding to the incremental load vector as given in Eq. 4 at the $(j+1)^{\text{th}}$ Newton-Raphson iteration.

$$K_i^j . \Delta q^{j+1} = Q_{ext}^{j+1} - Q^j \quad (4)$$

The cross-section strain vector at each Gaussian integration point (\hat{d}) is determined through shape functions and kinematic relations. Cubic Hermitian shape functions are employed to define transverse displacement fields while a quadratic shape function was adopted for the axial deformation field. Choosing a quadratic displacement field for the axial deformation field eliminated the effect of membrane locking (Alemdar 2001). The incremental internal nodal load

vector is calculated by multiplying the element flexibility with the compatibility equation as shown in Eq. 5.

$$\Delta Q = \left(H_{11}^j \right)^{-1} \cdot V^j \quad (5a)$$

$$V^j = \int_0^{1L} N_{D1}^T \cdot \left[\hat{d}^{j+1} - d^j - f^j \cdot (D(Q^j) - D_{\Sigma}(d^j)) \right] \cdot dx \quad (5b)$$

$$H_{11}^j = \int_0^{1L} N_{D1}^{jT} \cdot f^j \cdot N_{d1}^j \cdot dx \quad (5c)$$

Force shape functions are then utilized to calculate cross-section resultants at each Gaussian integration point (D). A linear shape function was chosen to describe the axial force field along the element length. This allows axial force transfer between the steel tube and concrete core due to slip. The bending moment field was also defined using linear shape functions. However, geometric nonlinearity due to P - δ effects was also incorporated into the bending moment field. For this purpose, the linear bending moment field was modified by adding the resulting P - δ moments obtained by multiplying the axial force field with transverse deformation fields. Following the calculation of cross-section resultants, as given in Eq. 6, the cross-section equilibrium equation is solved to calculate the incremental cross-section strain vectors (d) corresponding to the cross-section stress resultants interpolated from nodal forces.

$$\Delta d = f^j \cdot (D(Q^{j+1}) - D_{\Sigma}(d^j)) \quad (6)$$

The material constitutive relations are updated based on incremental strains obtained from Eq. 6. In the final stage of the state determination process internal forces (R) are determined according to Eq. 7 given below.

$$R^{j+1} = \left(G^{j+1} \right)^T \cdot Q^{j+1} + \left(G_{sc}^{j+1} \right)^T \cdot q^{j+1} + \left(G^{j+1} + M_d^{j+1} - H_{12}^{j+1} \right)^T \cdot \left(H^{j+1} \right)^{-1} \cdot \left[\int_0^{1L} \left(N_{D1}^{j+1} \right)^T \cdot \left[\hat{d}^{j+1} - d^{j+1} - f^{j+1} \cdot (D(Q^{j+1}) - D_{\Sigma}(d^{j+1})) \right] \cdot dx \right] \quad (7a)$$

$$G^{j+1} = \int_0^{1L} N_{D1}^{j+1T} \cdot N_{\hat{d}}^{j+1} \cdot dx \quad (7b)$$

$$G_{sc}^{j+1} = \int_0^{1L} N_{\hat{d}_{sc}}^{j+1T} \cdot k_{sc}^{j+1} \cdot N_{\hat{d}_{sc}}^{j+1} \cdot dx \quad (7b)$$

$$H_{12}^{j+1} = \int_0^{L} N_{D1}^{j+1T} \cdot f^{j+1} \cdot N_{D2}^{j+1} \cdot dx \quad (7c)$$

In the current formulation both geometrically and materially nonlinear effects were accounted for. A distributed plasticity approach was adopted to capture material inelasticity. The cross-sections along the element length were divided into individual steel and concrete fibers. The stress vs. strain response of each fiber is monitored throughout the analysis. In this research, comprehensive cyclic constitutive relations, modified and improved for RCFT members, were implemented to model stress vs. strain response of the concrete core and steel tube.

The cyclic concrete model proposed by (Chang and Mander 1994) was adopted accounting for typical behavioral characteristics of concrete observed in RCFT tests. The concrete model consisted of three types of polynomial curves including envelope curves, connecting curves, and transition curves. The envelope curves are assumed to be the backbones of the cyclic response. Based on the experimental observations by (Inai and Sakino 1996), the concrete core confined by the steel tube was assumed behave as plain concrete until its peak strength. Due to the inefficiency of the steel tube in confining the concrete as a result of its multiaxial stress state and flexibility of steel tube walls, no enhancement in concrete strength was assumed (Hajjar and Gourley 1997). An envelope curve in compression was derived having a nonlinear pre-peak region, a linear strength degradation region following the attainment of peak strength, and also a constant stress region at high strain levels. The unloading slope of the strength degradation region (K_c) and the stress level at constant strength region (f_{rc}) were represented through equations derived based on the stress-strain data of concrete provided by (Sakino and Yuping 1994) and (Varma 2000) as given in Eqs. 8 and 9 in terms of parameters of depth (D) over thickness (t) ratio of steel tube, compressive strength of concrete (f'_c), yield strength of steel tube (f_y), and modulus of elasticity of steel tube (E_s).

$$\frac{K_c}{f'_c} = 332.75 \times R - 9.60 \quad (8)$$

$$\frac{f_{rc}}{f'_c} = 0.32 \times R^{-0.5} \leq 0.85 \quad \text{where} \quad R = \frac{D}{t} \times \sqrt{\frac{f_y}{E_s}} \times \frac{f'_c}{f_y} \quad (9)$$

Connecting curves representing the loading and unloading branches between the positive and negative envelope curves, transition curves providing the rule to shift from one connecting curve to the other going in the opposite direction, and envelope curves in tension were taken as it is from (Chang and Mander 1994). The cyclic rules by (Chang Mander 1994) augmented with the negative envelope curves derived in this research are thus capable of simulating the key features of RCFT members attributed to the cyclic behavior of concrete core including strength degradation, reduction in elastic zone, and reduction in stiffness. (Chang and Mander 1994) also provided unique rules in simulating transition from tension into compression. In addition, crack closing and opening are modeled by identifying the difference in response before and after attaining the cracking strain.

The uniaxial bounding surface model by (Mizuno et al. 1992) is implemented in this research to simulate the cyclic response of the cold formed steel tube of RCFT members. (Mizuno et al. 1992) defined an outer bounding surface and an inner loading surface. The bounding surface was introduced to account for the fact that plastic modulus attains a limiting value as cyclic loading proceeds. The loading surface represents the boundary between elastic and plastic response. Once the stress point reaches the loading surface, plastic deformation initiates and the plastic modulus softens based on the distance between loading and bounding surfaces. (Mizuno et al. 1992) also introduced intermediate surfaces including memory surface and virtual bounding surface to ensure a gradual reduction in plastic modulus. In this research the ability to simulate local buckling of the steel tube was added to the steel model (Hajjar and Gourley 1997, Varma 2000). It was assumed that once the strain level reaches the limiting value of local buckling, a strength degradation region initiates and the strength degradation region is followed by a constant stress region at high strain levels. The strain level at initiation of local buckling (ϵ_{lbf}) normalized by yield strain of steel tube (ϵ_y) was derived from axially loaded RCFT column tests as given in Eq. 10.

$$\frac{\epsilon_{lbf}}{\epsilon_y} = 3.14 \times \left(\frac{D}{t} \times \sqrt{\frac{f_y}{E_s}} \right)^{-1.48} \quad (10)$$

The parameters defining the slope of the strength degradation region after local buckling (K_s) and the constant stress level at high strain values (f_{rs}) were determined based on a calibration study performed on axially loaded RCFT specimens with wide ranges of material strength and geometric properties as given in Eq. 11 and 12, respectively.

$$\frac{K_s}{f_y} = 0, \frac{D}{t} \frac{f_y}{E_s} \leq 0.08 \text{ and } \frac{K_s}{f_y} = 1033.50 \frac{D}{t} \frac{f_y}{E_s} - 86.32, \frac{D}{t} \frac{f_y}{E_s} \geq 0.08 \quad (11)$$

$$\frac{f_{rs}}{f_y} = 1, \frac{D}{t} \frac{f_y}{E_s} \leq 0.08 \text{ and } \frac{f_{rs}}{f_y} = -7.31 \frac{D}{t} \frac{f_y}{E_s} + 1.58, \frac{D}{t} \frac{f_y}{E_s} \geq 0.08 \quad (12)$$

Verification of Geometrically Nonlinear Materially Linear Problems

A variety of benchmark problems were selected from the literature in order to assess the accuracy of the formulation for geometrically nonlinear and materially linear problems. As an example, the Harrison portal frame was analyzed under constant axial load and linearly increasing lateral load (Clarke et al. 1993). Columns were modeled as 18 DOF RCFT members while girders were modeled as 12 DOF steel members. RCFT column members were modeled using 1 and 3 elements along its length. The axial and flexural stiffness ratio of the steel tube and concrete core were kept to be equal in all of the analyses. The comparison of the theoretical and computational lateral load vs. lateral deformation response of the portal frame can be seen in Figure 1. It can be seen that as the number of elements used for RCFT columns increases, a better correlation is obtained with the theoretical results.

Verification of Geometrically Nonlinear and Materially Nonlinear Problems

The first set of verification examples was selected from proportionally loaded specimens where simply supported RCFT columns are tested under linearly increasing axial load with constant eccentricity. The specimens tested by (Bridge 1976), (Shakir-Khalil and Zeghiche 1989), and (Cederwall et al. 1990) covering a wide range of material and geometric properties were analyzed and good correlation was attained with the experimental results as can be seen from Figure 2 [Specimens 1, 1*, 2, 7, 10, and 13 have values, respectively, of $D/t = 24, 20, 24, 24, 15, 15$; $L/D = 25, 10, 34, 34, 25, 25$; $f'_c = 6.8, 4.3, 5.8, 6.4, 5.6, 11.4$ ksi; $f_y = 44, 42, 56, 57, 55, 57$ ksi; L is the length of the RCFT]. For proportionally loaded specimens, slip between the steel tube and concrete core was found to be insignificant. As an example, for Specimen 1 tested by (Cederwall et al. 1990), the maximum differential axial displacement at mid-height was approximately 0.000037 inches.

To verify the capability of the analysis model for non-proportionally loaded RCFT beam-columns, a verification example was selected from the specimens tested by (Sakino and Tomii 1981). The specimen selected for analysis was tested under constant axial load and cyclically applied shear loading. Since the specimen had fixed boundary conditions both at the top and bottom supports, differential axial displacement between steel tube and concrete core is expected to be insignificant. Therefore, slip between steel tube and concrete core was prevented using penalty functions. Based on the analysis results by (Hajjar et al. 1998), it was found that local buckling of steel tube in RCFT specimens tested under flexure takes place at a higher strain level than RCFT specimens tested under pure compression. Therefore, a relative plastic strain limit of 0.012 was found to correlate well with the strain levels at which local buckling was experimentally observed for the specimens with D/t ratio of 24 and 34 by (Sakino and Tomii 1981) and is established in this work to provide a realistic assessment of the local buckling strain for RCFT subjected to a combination of axial force and flexure. The comparison of experimental and computational results is presented in Figure 3 and a good correlation was attained.

In future work, the proposed constitutive relations will be calibrated further with respect to multiple specimens from the literature with comprehensive material properties and geometric dimensions as well as with different loading schemes. This will allow us to reduce and quantify the uncertainty in our capacity assessments related to modeling assumptions.

Conclusions

In this paper, various numerical tools were presented to quantify the capacity of RCFT members and frames. An experimental database was constructed and experimental results of RCFT members were documented in detail. Using the available experimental data, damage function equations were proposed to calculate the available capacity of RCFT members. A new mixed finite element formulation for modeling of RCFT members is proposed and it is implemented in a general purpose analysis program allowing both static and dynamic analysis of structures. Comprehensive and efficient constitutive models of the steel tube and concrete core were developed and implemented successfully, and the results demonstrate that the proposed finite element formulation is capable of predicting the response of RCFT members under both monotonically and cyclically applied loadings. The proposed finite element formulation

augmented with the constitutive relations developed in this research will be used in demand and capacity assessment of RCFT composite frames in future research.

Acknowledgments

This research was funded by the National Science Foundation (Grant No. CMS-0084848) under Dr. Vijaya Gopu and by the University of Minnesota. Any opinions, findings, and conclusions or recommendations expressed in this material are those of the authors and do not necessarily reflect the views of the National Science Foundation.

Figures

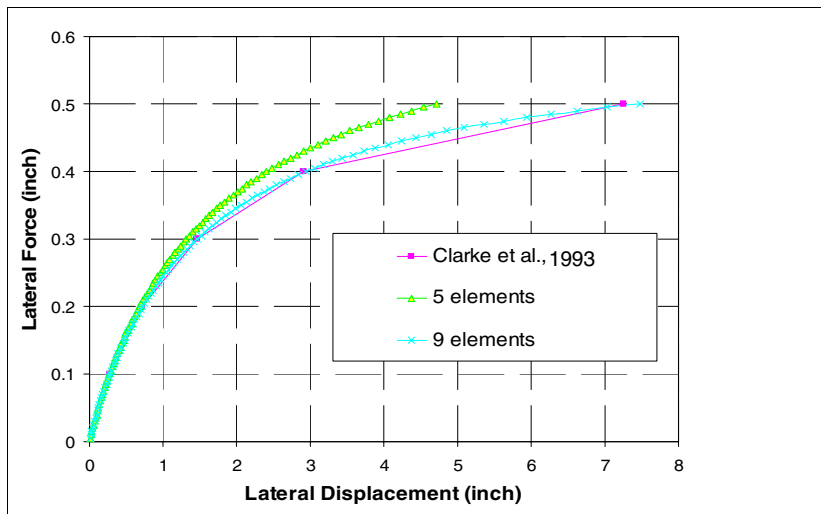


Figure 1. Computational vs. theoretical response of portal frame with RCFT columns and steel girder.

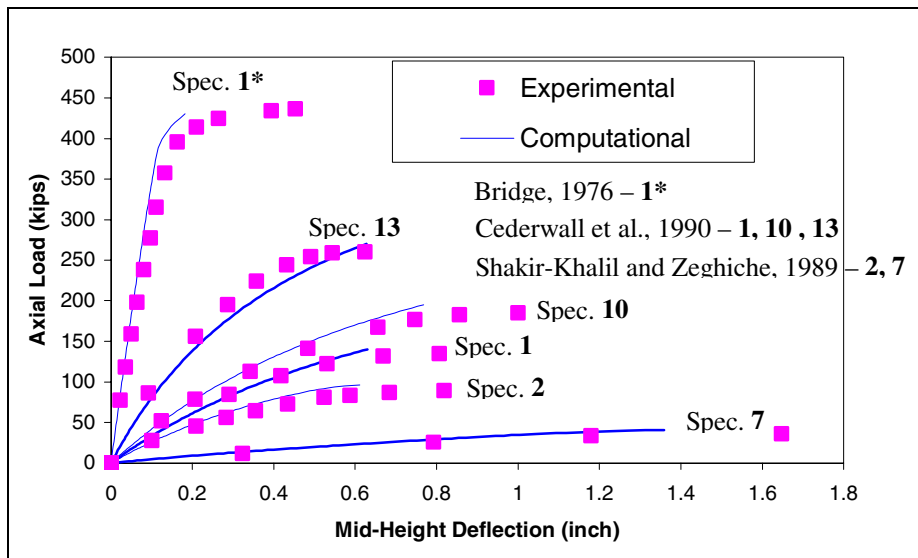


Figure 2. Comparison of experimental and computational results for proportionally-loaded RCFT beam-column.

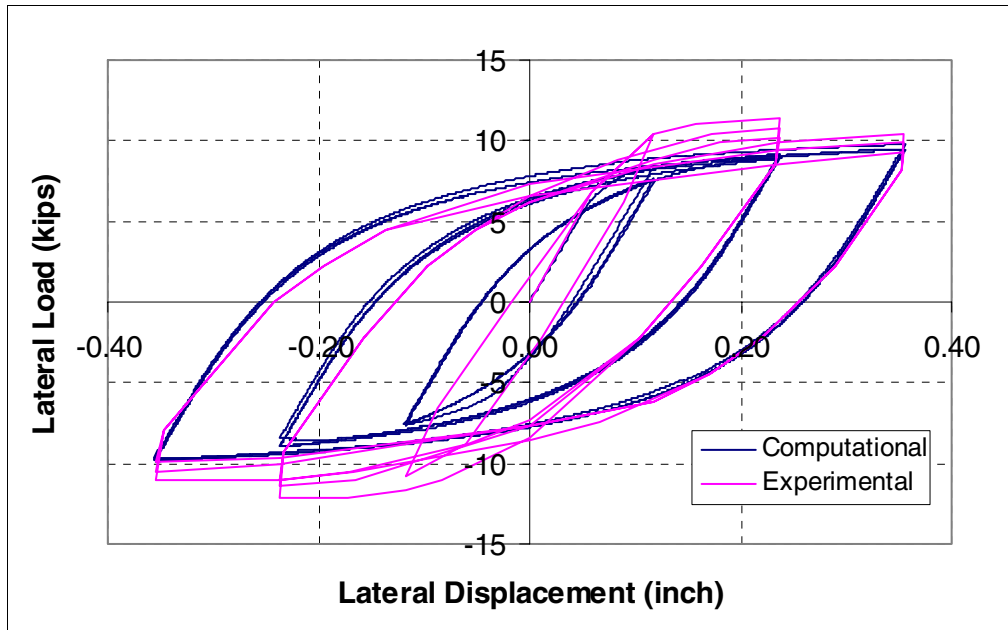


Figure 3. Comparison of experimental and computational results for non-proportionally loaded RCFT beam-column

Appendix

- D_{sc} Stress resultant vector of the steel-concrete interface
- D_{Σ} Stress resultant vector from constitutive relations
- K_t Tangent stiffness
- M_d Matrix resulting from linearization of the compatibility equation
- N_{D1} Shape function matrix for cross-section forces ($D = N_{D1} \cdot Q$)
- N_{D2} Matrix resulting from variation of D ($\delta N_{D1} \cdot Q = N_{D2} \cdot \delta q$)
- $N_{\delta \hat{d}}$ Matrix resulting from variation of \hat{d} ($\delta \hat{d} = N_{\delta \hat{d}} \cdot q$)
- $N_{\delta \hat{d}_{sc}}$ Matrix resulting from variation of \hat{d}_{sc} ($\delta \hat{d}_{sc} = N_{\delta \hat{d}_{sc}} \cdot q$)
- Q_{ext} External load vector
- \hat{d}_{sc} Strain vector of the steel and concrete interface
- f Cross-section flexibility matrix

References

- Alemdar, B.N., 2001. Distributed Plasticity Analysis of Steel Building Structural Systems, *Ph.D. Thesis*, Georgia Institute of Technology, Atlanta, GA.
- Bridge, R. Q., 1976. Concrete Filled Steel Tubular Columns, Report No. R283, School of Civil Engineering, University of Sydney, Sydney, Australia.
- Cederwall, K., Engstrom, B., and Grauers, M., 1990. High Strength Concrete Used in Composite

- Columns, 2nd Intl. Symp. on Util. of High-Str. Conc., ACI, Detroit, MI, 195-214.
- Chang, G. A. and Mander, J. B., 1994. Seismic Energy Based Fatigue Damage Analysis of Bridge Columns: Part I – Evaluation of Seismic Capacity, Report No. NCEER-94-0006, State University of New York, Buffalo, NY.
- Clarke, M. J., Bridge R. Q., Hancock, G. J., and Trahir, N. S., 1993. Benchmarking and Verification of Second-Order Elastic and Inelastic Frame Analysis Programs, *Plastic Hinge Based Methods for Advanced Inelastic Analysis and Design of Steel Frames*, White, D. W. and Chen, W. F. (eds.), SSRC, Bethlehem, PA.
- Hajjar, J. F., 2002. Composite Steel and Concrete Structural Systems for Seismic Engineering, *Journal of Constructional Steel Research* 58 (5-8), 703-723.
- Hajjar, J. F. and Gourley, B. C., 1997. A Cyclic Nonlinear Model for Concrete-Filled Tubes. I. Formulation, *Journal of Structural Engineering*, ASCE 123 (6), 736-744.
- Hajjar, J. F., Molodan, A., and Schiller, P. H., 1998. A Distributed Plasticity Model for Cyclic Analysis of Concrete-Filled Steel Tube Beam-Columns and Composite Frames, *Engineering Structures* 20 (4-6), 398-412.
- Inai, E. and Sakino, K., 1996. Simulation of Flexural Behavior of Square Concrete Filled Steel Tubular Columns, Proc. Third Joint Tech. Coord. Comm. Mtg., U.S.-Japan Coop. Res. Prog., Phase 5: Comp. and Hybrid Struct., Hong Kong, December 12-14, 1996, NSF, Arlington, VA.
- Mizuno, E., Shen, C., Tanaka, Y., and Usami, T., 1992. A Uniaxial Stress-Strain Model for Structural Steels under Cyclic Loading, Stability and Ductility of Steel Structures Steels under Cyclic Loading, Fukumoto, Y. and Lee, G. C. (eds.), CRC Press, Boca Raton, FL, 37-48.
- Nukala, P.K.V.V. and White, D.W., 2003. Variationally Consistent State Determination Algorithms for Nonlinear Analysis Using Mixed Rod Finite Element Formulations, *Computational Methods in Applied Mechanics and Engineering* 193, 3647-3666.
- OpenSEES, 1999. Open System For Earthquake Engineering Simulation, Pacific Earthquake Engineering Research Center, University of California at Berkeley, Berkeley, CA.
- Sakino, K. and Yuping, S., 1994. Stress-strain Curve of Concrete Confined by Rectilinear Hoop, *Journal of Structural Construction Engineering*, AIJ, No. 461, July, 95-104.
- Sakino, K. and Tomii, M., 1981. Hysteretic Behavior of Concrete Filled Square Steel Tubular Beam-Columns Failed in Flexure, *Transactions of the Japan Concrete Institute* 3, 439-469.
- Shakir-Khalil, H. and Zeghiche, Z., 1989. Experimental Behavior of Concrete-Filled Rolled Rectangular Hollow-Section Columns, *The Structural Engineer* 67 (19), 345-353.
- Tort, C. and Hajjar, J. F., 2004. Damage Assessment of Rectangular Concrete-Filled Steel Tubes for Performance-Based Design, *Earthquake Spectra* 20 (4), 1317-1348.
- Varma, A. H., 2000. Seismic Behavior, Analysis, and Design of High Strength Square Concrete Filled Steel Tube (CFT) Columns, *Ph.D. Thesis*, Dept. of Civil Engrg., Lehigh Univ., Bethlehem, PA.